European Heart Journal (2012) **33**, 372–383
doi:10.1093/eurheartj/ehr387

In vivo characterization of coronary plaques: novel findings from comparing greyscale and virtual histology intravascular ultrasound and near-infrared spectroscopy

Jun Pu[1†], Gary S. Mintz[1], Emmanouil S. Brilakis[2], Subhash Banerjee[2], Abdul-Rahman R. Abdel-Karim[2], Brijeshwar Maini[3], Sinan Biro[1], Jin-Bae Lee[1], Gregg W. Stone[1], Giora Weisz[1], and Akiko Maehara[1*]

[1]Columbia University Medical Center and the Cardiovascular Research Foundation, 111 East 59th Street, New York, NY, USA; [2]VA North Texas Healthcare System and University of Texas Southwestern Medical Center at Dallas, Dallas, TX, USA; and [3]Pinnacle Health System, Harrisburg, PA, USA

Received 20 February 2011; revised 17 August 2011; accepted 27 September 2011; online publish-ahead-of-print 20 October 2011

Aims To test the hypothesis that near-infrared spectroscopy (NIRS) combined with intravascular ultrasound (IVUS) would provide novel information of human coronary plaque characterization.

Methods and results Greyscale-IVUS, virtual histology (VH)-IVUS, and NIRS were compared in 131 native lesions (66 vessels) that were interrogated during catheterization by all three modalities. Greyscale-IVUS detected attenuated and echolucent plaques correlated with NIRS-detected lipid-rich areas. Attenuated plaques contained the highest NIRS probability of lipid core, followed by echolucent plaques. By VH-IVUS, 93.5% of attenuated plaques contained confluent necrotic core (NC) and were classified as VH-derived fibroatheromas (FAs). Although 75.0% of echolucent plaques were classified as VH-FAs, VH-NC was seen *surrounding* an echolucent zone, but not *within any* echolucent zone; and echolucent zones themselves contained fibrofatty and/or fibrous tissue. All calcified plaques with arc $>90^{\circ}$ contained $>10\%$ VH-NC (range 16.0–41.2%) and were classified as calcified VH-FAs, but only 58.5% contained NIRS-detected lipid core. A positive relationship between VH-derived %NC and NIRS-derived lipid core burden index was found in non-calcified plaques, but not in calcified plaques.

Conclusion Combining NIRS with IVUS contributes to the understanding of plaque characterization *in vivo*. Further studies are warranted to determine whether combining NIRS and IVUS will contribute to the assessment of high-risk plaques to predict outcomes in patients with coronary artery disease.

Keywords Coronary disease • Intravascular imaging • Near-infrared spectroscopy

Introduction

Greyscale-intravascular ultrasound (IVUS) is widely used for quantifying plaque distribution and severity, but, beyond the assessment of calcification, is limited to tissue characterization, especially for lipid-containing plaque; and the meanings of the greyscale-IVUS findings of echolucency and attenuation are not clear.[1] Intravascular ultrasound radiofrequency data analysis, known as virtual histology IVUS (VH-IVUS), has been developed to improve on the plaque characterization of greyscale-IVUS and colour-coded plaque as either white (dense calcium, DC), red (necrotic core, NC), light-green (fibrofatty, FF), or dark-green (fibrous tissue, FT).[2]

Near-infrared spectroscopy (NIRS) is routinely used to characterize chemical composition of biological tissue.[3] The ability of NIRS to discriminate lipid-rich atherosclerotic plaque with high sensitivity and specificity *in vitro*[4] provides the possibility that NIRS can be used

* Corresponding author. Tel: +1 646 434 4569, Fax: +1 646 434 4464, Email: amaehara@crf.org
† Present address: Renji Hospital, School of Medicine, Shanghai Jiaotong University, Shanghai, China.

to detect lipid-rich atheromas *in vivo*.[5] The major limitation of NIRS is that it provides compositional, but not structural, information.

The purpose of the present study was to use NIRS and VH-IVUS in comparison with greyscale-IVUS to better understand plaque morphology, morphometry, and composition. In particular, we evaluated three greyscale-IVUS findings that have been related to coronary disease prognosis: echolucent plaques and attenuated plaques have been associated with a more unstable clinical course, whereas calcified plaque has been associated with a more stable course.[6–9]

Methods

Study population

From October 2008 through February 2010, we conducted a study to compare the *in vivo* characterization of coronary plaques among greyscale and VH-IVUS and NIRS. Patients were recruited from the population undergoing elective percutaneous coronary intervention (PCI) of native *de novo* coronary lesions for stable coronary artery disease or acute coronary syndrome (ACS). Each lesion selected for imaging was a culprit or target lesion undergoing planned PCI. Patients were excluded if they were pregnant or nursing, if life expectancy was <2 years, or if target vessels were coronary artery bypass grafts. Data of angiograms, NIRS, and IVUS were prospectively entered into the study database. Overall, greyscale and VH-IVUS and NIRS were performed in 78 consecutive patients (91 vessels). Sixteen vessels (12 patients) required pre-dilation prior to imaging and were excluded; and 9 vessels (7 patients) were excluded because of poor quality of IVUS ($n = 3$) or NIRS ($n = 4$) images. Thus, 66 vessels from 59 patients were included in the final analysis. No patient developed angina or had any complication (i.e. distal embolization, no-reflow, or thrombus formation) during IVUS and NIRS imaging, both of which were performed after intracoronary administration of nitroglycerin (100–200 μg). The greyscale-IVUS analysis, the VH analysis, and the NIRS analysis were performed without knowledge of the findings obtained from the other two methods.

This study was performed in accordance with the Code of Federal Regulations and the Declaration of Helsinki. The study protocol was approved by the Institutional Review Board. Informed consent was obtained from all patients before the procedure.

Intravascular ultrasound image acquisition and analysis

An Eagle Eye 20 MHz, 3.2Fr phased-array catheter (Volcano Corporation, Rancho Cordova, CA, USA) was advanced into the distal coronary artery and withdrawn to the aorta by motorized pullback (0.5 mm/s). During pullback, greyscale-IVUS was recorded, raw radiofrequency data were captured at the peak R-wave, and reconstruction of the colour-coded map by a VH-IVUS data recorder was performed. Image data were archived onto DVD and sent to the Cardiovascular Research Foundation, NYC, NY, for off-line analyses.

Greyscale analyses were performed using the validated planimetry software (EchoPlaque, INDEC Systems, Inc., Mountain View, CA, USA). Criteria for inclusion of a plaque in the study database were maximal plaque thickness ≥ 0.5 mm and plaque burden $\geq 40\%$, at least 1.5 mm in length, on greyscale-IVUS.[10,11] Quantitative measurements were done according to criteria from the American College of Cardiology (ACC) consensus statement on IVUS.[12] Qualitative assessments of greyscale-IVUS plaque morphology were based on the echogenic characteristics of the plaque on the cross-sectional view, and the adventitia was used as a reference for echoreflectivity.[12] We emphasized three greyscale-IVUS plaque types: intraplaque echolucent zone (echolucent plaque); plaque with backward attenuation despite the absence of calcification (attenuated plaque); and calcified plaque. Echolucent plaque was defined as a large echolucent zone (thickness >0.3 mm) surrounded by tissue of greater echogenicity that was closer to the luminal surface than to the adventitia (shallow location).[6,12] Attenuated plaque was defined as plaques with $>30^\circ$ ultrasonic attenuation (attenuation of deeper arterial structures) despite the absence of bright calcium.[7,8] Calcified plaque was defined as hyperechoic plaque occupying $>90^\circ$ of arc with acoustic shadowing.[9,12] Control plaque was defined as plaques with echogenicity similar to the adventitia, but without an echolucent zone, attenuation, or calcification.[12]

VH-IVUS analyses were performed using the Volcano Image Analysis software (Version 3.0; Volcano Corporation, Rancho Cordova, CA, USA). The qualitative assessment scheme for VH-IVUS lesion types is based on the percentages of the four different plaque components. Lesions were classified as: VH thin-cap fibroatheroma (VH-TCFA), thick-cap fibroatheroma (ThCFA), pathological intimal thickening (PIT), fibrotic plaque, or fibrocalcific plaque.[13] Determination was based on the observations of two independent reviewers (J.P. and A.M.) who were blinded to patient characteristics. If the initial classification differed between the two individuals, the final classification was achieved by consensus.

Near-infrared spectroscopy image acquisition and analysis

Using the same protocol as for IVUS imaging, a 3.2Fr InfraReDx (Burlington, MA, USA) NIRS catheter was advanced into the distal coronary vessel. Automated mechanical pullback was performed at a speed of 0.5 mm/s and 240 rotations per minute until the NIRS catheter entered the guiding catheter. Raw spectra were acquired at a rate of $\sim$40 Hz (one spectrum every 25 ms). Spatial filtering and image processing of the raw data produced an image with data points every 0.1 mm and every 1°.

During catheter pullback, the measurement of the probability of lipid core is displayed as an NIRS 'chemogram' (*Figure 1*, top), a digital colour-coded map of the location and intensity of lipid core, with the *X*-axis indicating the pullback position in millimetres (every 0.1 mm) and the *Y*-axis indicating the circumferential position in degrees (every 1°) as if the coronary vessel has been split open along its longitudinal axis. Spectroscopic information at each pixel is transformed into a probability of lipid core that is then mapped to a 128 (7-bit) red-to-yellow colour scale, with the low probability of lipid shown as red and the high probability of lipid shown as yellow. If a pixel does not contain enough data (e.g. as caused by guidewire shadowing), it appears black—i.e. a 'non-viable' pixel.

The 'block chemogram' (*Figure 1*, bottom) is a summary metric that is computed to display the probability that a lipid core plaque (LCP) is present for all measurements using the top 10th percentile pixel information (i.e. the 90th percentile value) of the corresponding 2 mm NIRS 'chemogram' segment. If the probability of the top 10th percentile is ≥ 0.98, the entire block is assigned yellow; if the probability of the top 10th percentile is 0.84–0.98, the entire block is assigned tan; if the probability of the top 10th percentile is 0.57–0.84, the entire block is assigned orange; if the probability of the top 10 percentile is <0.57, the entire block is assigned red. The 'block chemogram' provides a summary of the data to enhance interpretation of the chemogram and does not indicate individual pixel data or the location of a measurement in the circumferential dimension.

Near-infrared spectroscopy image analyses were performed off-line using the in-house, Matlab-based software programmed at the

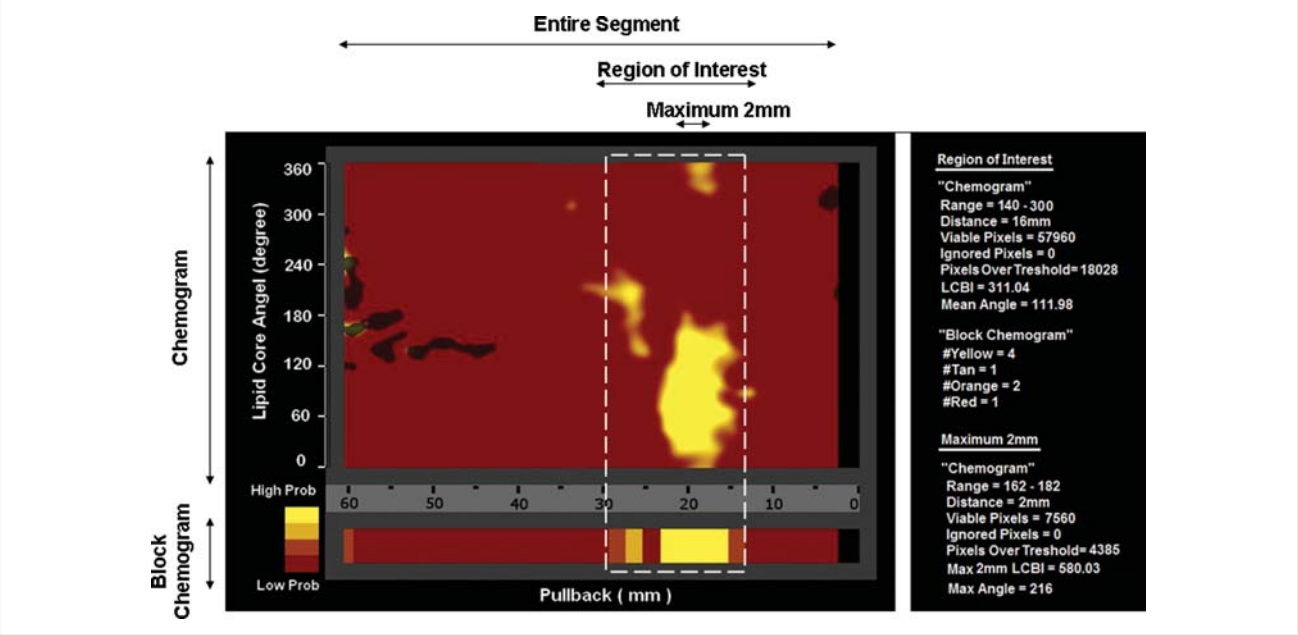

Figure 1 Example of near-infrared spectroscopy. Top, near-infrared spectroscopy 'chemogram': a digital colour-coded map of the artery wall indicating the location and intensity of lipid core in the region of interest (ROI), with the *X*-axis indicating the pullback position (in mm) and the *Y*-axis, the circumferential position of the measurement (in degrees). The chemogram is presented as if the coronary vessel has been split open along its longitudinal axis. Bottom, near-infrared spectroscopy 'block chemogram': summary of the presence of lipid core at 2 mm intervals in four probability categories (left, probability of the lipid core: yellow > tan > orange > red). Image interpretation: in the near-infrared spectroscopy 'chemogram', a prominent lipid core signal is detected in the coronary vessel (range 14–30 mm; distance 16 mm). The lipid core burden index (LCBI) of ROI (white rectangles) is 311.0, with a mean angle of lipid core of 112.0°. The maximum 2 mm LCBI is 580.0, and the maximum angle of lipid core is 216°. In the 'block chemogram', the ROI contains four yellow (50%), one tan (12.5%), two orange (25%), and one red (12.5%) blocks, indicating high probability of the lipid core presence.

Cardiovascular Research Foundation, which read the information of each pixel and counted total viable and non-viable pixels. The presence of lipid core within the region of interest required at least one yellow block (95% specificity that lipid core was present).[5] Yellow pixels (pixels above the preset threshold for the detection of LCP) within the analysed segment were divided by all viable pixels in the 'chemogram' to generate the lipid core burden index (LCBI) per mille (‰). Total LCBI, the 2 mm length with the maximum LCBI, and mean and maximum angles of lipid core were computed using the entire spectroscopic information within the region of interest in the 'chemogram' and exported by the NIRS software automatically.

Registering intravascular ultrasound and near-infrared spectroscopy images

Important angiographic landmarks during the pullback were imprinted on the chemogram—i.e. starting NIRS position, starting position of target lesion, side branches, and distal edge of the guiding catheter, etc. Those same landmarks were also bookmarked on the IVUS images. Near-infrared spectroscopy images were matched to IVUS images using known landmarks on both modalities and with the aid of interpolated lengths calculated using catheter pullback speeds. Because each chemogram block measured 2 mm in length, separate lipid cores (on NIRS) required three consecutive non-yellow chemogram blocks between yellow chemogram blocks, whereas separate greyscale and VH-IVUS lesion types required 6 mm separation between them.

Statistical analysis

Data analyses were performed using SPSS version 12.0 (SPSS, Inc., Chicago, IL, USA) and SAS version 9.1 (SAS Institute, Inc., Cary, NC, USA). For patient-level data, categorical data were expressed as absolute values and percentages and compared using χ^2 or Fisher's exact test, and continuous data were reported as median (inter-quartile range, IQR) and compared using Kruskal–Wallis/Wilcoxon rank-sum tests. For lesion-level data, a model with generalized estimating equation (GEE) approach was used to compensate for any potential cluster effect of multiple lesions in the same individual.[14] The correlation between VH-IVUS-derived parameters vs. NIRS-derived parameters was analysed using Spearman correlation coefficients. *P*-values were adjusted with the GEE method for repeated measures. Inferential statistical tests were conducted at the significance level of 0.05.

Results

Patient characteristics

Baseline patient characteristics are shown in *Table 1*. The length of the artery imaged was 93.4 ± 20.8 mm in the left anterior descending artery (LAD) to the ostium of the left main coronary artery (LMCA), 67.9 ± 17.5 mm in the left circumflex (LCX) to the ostium of the LMCA, and 94.4 ± 26.4 mm in the right coronary (RCA) to its ostium.

Table 1 Clinical characteristics (patients = 59; vessels = 66)

Characteristic	Value
Age, years	61 (57–68)
Male, *n* (%)	54 (91.5)
Medical history, *n* (%)	
Current smoker	22 (37.3)
Hypertension	55 (93.2)
Diabetes mellitus	25 (42.4)
Dyslipidaemia	53 (89.8)
Prior myocardial infarction	24 (40.7)
Prior coronary bypass	11 (18.6)
Family history	28 (47.5)
Clinical presentation, *n* (%)	
Non-ST-elevation myocardial infarction	12 (20.3)
Unstable angina	14 (23.7)
Stable angina	31 (52.5)
Atypical chest pain	2 (3.4)
Target vessel, *n* (%)	
Left anterior descending	32 (48.5)
Left circumflex	16 (24.2)
Right coronary artery	18 (27.3)

Data are presented as median (IQR) or number (%).

Overall greyscale and virtual histology-intravascular ultrasound findings

A total of 131 plaques in 66 vessels that met all inclusion criteria were included into the study database. From the database, we identified 16 echolucent plaques in 13 vessels (6 LAD, 3 LCX, and 4 RCA); 31 attenuated plaques in 26 vessels (11 LAD, 6 LCX, and 9 RCA); 41 calcified plaques in 31 vessels (17 LAD, 6 LCX, and 8 RCA), and 30 control plaques in 30 vessels (15 LAD, 8 LCX, and 7 RCA). Virtual histology-IVUS findings are summarized in *Table 2*. Overall, VH-derived %NC was 23.5% (IQR 17.4–29.6%) with a maximum %NC of 34.5% (IQR 27.4–38.6%). The mean NC angle was 62.5° (IQR 27.3–106.8°) with a maximum NC angle of 101.0° (IQR 54.5–191.5°).

Overall near-infrared spectroscopy findings

Near-infrared spectroscopy findings are summarized in *Table 2*. Overall, lipid core was detected in 75 lesions (57.3%) in 41 vessels (20 LAD, 10 LCX, and 11 RCA). In the 'chemogram', the overall LCBI was 101.2 (IQR 31.4 –237.5) with a mean lipid core angle of 39.3° (IQR 16.3–89.3°). In the 'block chemogram', there were 15.1% yellow blocks (highest probability of lipid core) and 60.1% red blocks (lowest probability of lipid core). The proportion of tan and orange blocks—indicating that lipid core was present, but with a probability less than that of yellow—were 9.2 and 15.7%, respectively. Overall, there was no significant correlation between LCBI and plaque burden (Rho = 0.26, $P = 0.103$).

Table 2 Virtual histology-intravascular ultrasound and near-infrared spectroscopy findings (plaques = 131)

Characteristic	Median (IQR)
VH-IVUS parameters	
Mean NC area (mm^2)	0.9 (0.4–1.9)
Mean FF area (mm^2)	0.7 (0.4–1.4)
Mean FT area (mm^2)	3.7 (1.7–5.7)
Mean DC area (mm^2)	0.3 (0.1–0.6)
%NC	23.5 (17.4–29.6)
%FF	10.8 (6.5–16.1)
%FT	49.6 (42.7–60.9)
%DC	10.7 (5.5–19.1)
Mean angle of NC (degree)	62.5 (27.3–106.8)
Maximum angle of NC (degree)	101.0 (54.5–191.5)
NIRS parameters	
LCBI	101.2 (31.4–237.5)
Maximum 2 mm LCBI	157.9 (57.5–322.3)
Mean angle of LCP (degree)	39.3 (16.3–89.3)
Maximum angle of LCP (degree)	83.0 (35.0–137.0)

Data are expressed as median (IQR).
DC, dense calcium; FF, fibrofatty; FT, fibrotic tissue; LCBI, lipid core burden index; LCP, lipid core plaques; NC, necrotic core; NIRS, near-infrared spectroscopy; VH, virtual histology.

Attenuated plaques

As shown in *Figure 2*, attenuated plaques had a greater remodelling index and were more eccentric compared with control plaques.

As shown in *Figure 3* and compared with control plaques, attenuated plaques had more %NC ($P < 0.001$) as well as more VH-derived FAs (93.5 vs. 60.0%, $P = 0.002$) and VH-derived TCFAs (45.2 vs. 20.0%, $P = 0.041$). However, there were similar amounts of NC [26.0% (22.1–31.3%) vs. 27.8% (22.3–34.5%), $P = 0.762$] when comparing calcified vs. attenuated plaques. Qualitatively, most (93.5%) attenuated plaque contained confluent NC when analysed by VH-IVUS; an example is shown in *Figure 4*.

On NIRS analysis, 90.3% of attenuated plaques contained lipid core as identified by the presence of at least one yellow block on the block chemogram (*Figure 5*). As shown in *Figure 6*, compared with control plaques, attenuated plaques had a higher LCBI, a larger maximum 2 mm LCBI, and a greater mean and maximum angles of lipid core (all $P < 0.001$). Similarly, there were a significantly higher LCBI, maximum 2 mm LCBI, and mean angle and maximum angles of lipid core in attenuated vs. calcified plaques (all $P < 0001$). As shown in *Figure 7*, the probability of lipid core was highest in attenuated plaques, as indicated by the greatest percentage of yellow blocks.

Echolucent plaques

As shown in *Figure 2*, there was a higher eccentricity index in echolucent plaques when compared with control plaques ($P = 0.005$).

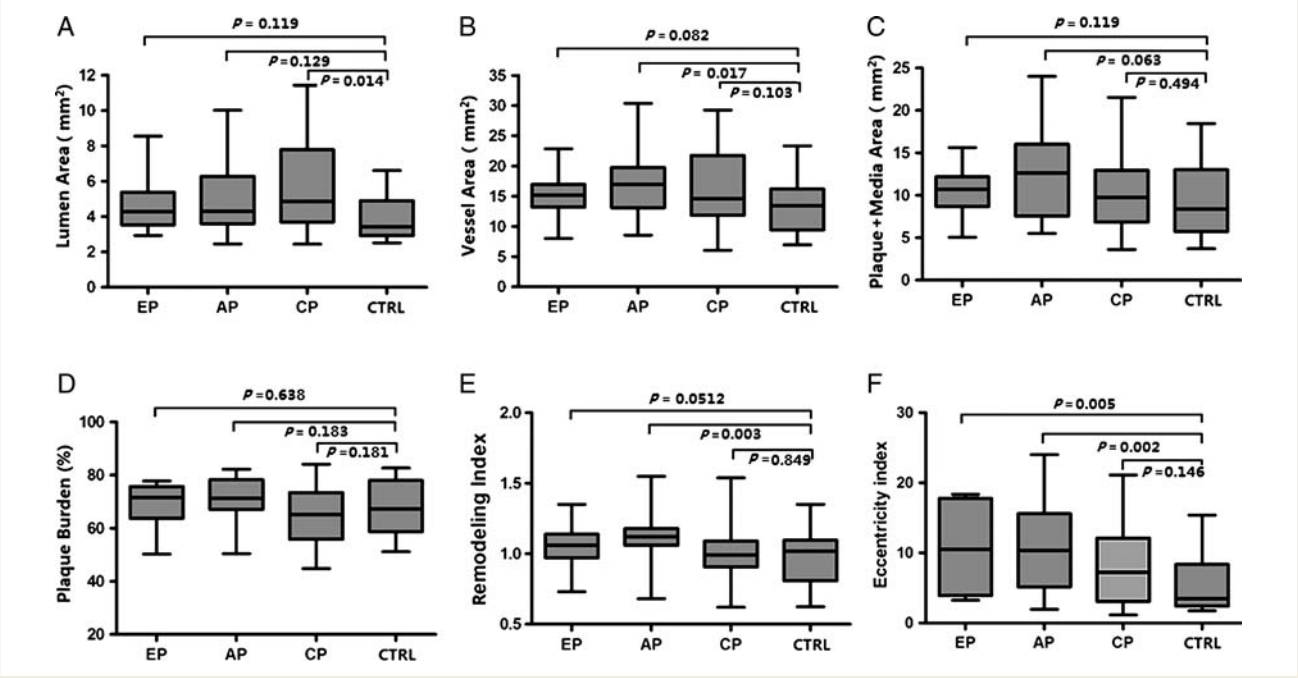

Figure 2 Baseline morphometric greyscale-intravascular ultrasound results of different groups. Lumen area (*A*), vessel area (*B*), plaque and media area (*C*), plaque burden (*D*), remodelling index (*E*), and eccentricity index (*F*) in echolucent plaque (EP), attenuated plaque (AP), calcified plaque (CP) groups were compared with those in the control plaque (CTRL) group.

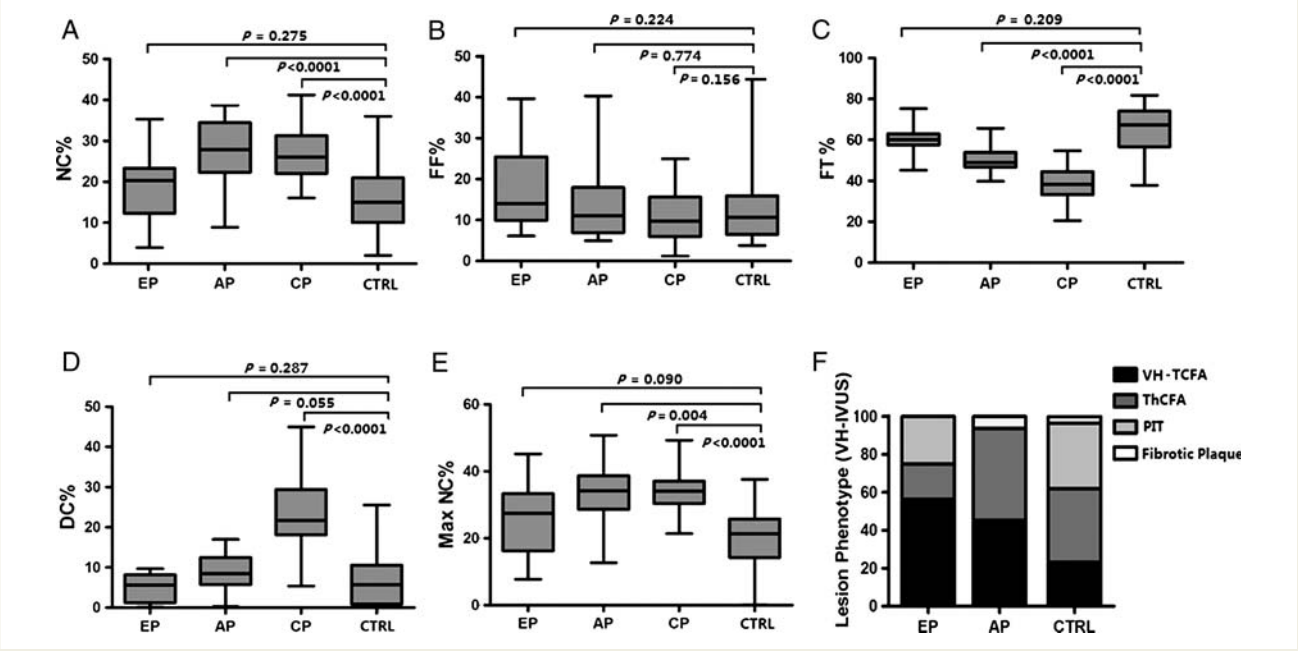

Figure 3 Relationship between greyscale-intravascular ultrasound plaque types and virtual histology findings. (*A*–*E*) Mean percentage of the four virtual histology-intravascular ultrasound plaque components, including necrotic core (NC, A), fibrofatty (FF, B), fibrous tissue (FT, C), and dense calcium (DC, D) as well as the maximum %NC (Max NC%, E) in echolucent plaque (EP), attenuated plaque (AP), calcified plaque (CP) groups were compared with those in control plaque (CTRL) group. (*F*) Percentages of virtual histology-derived lesion phenotypes in EP, AP, and CTRL groups.

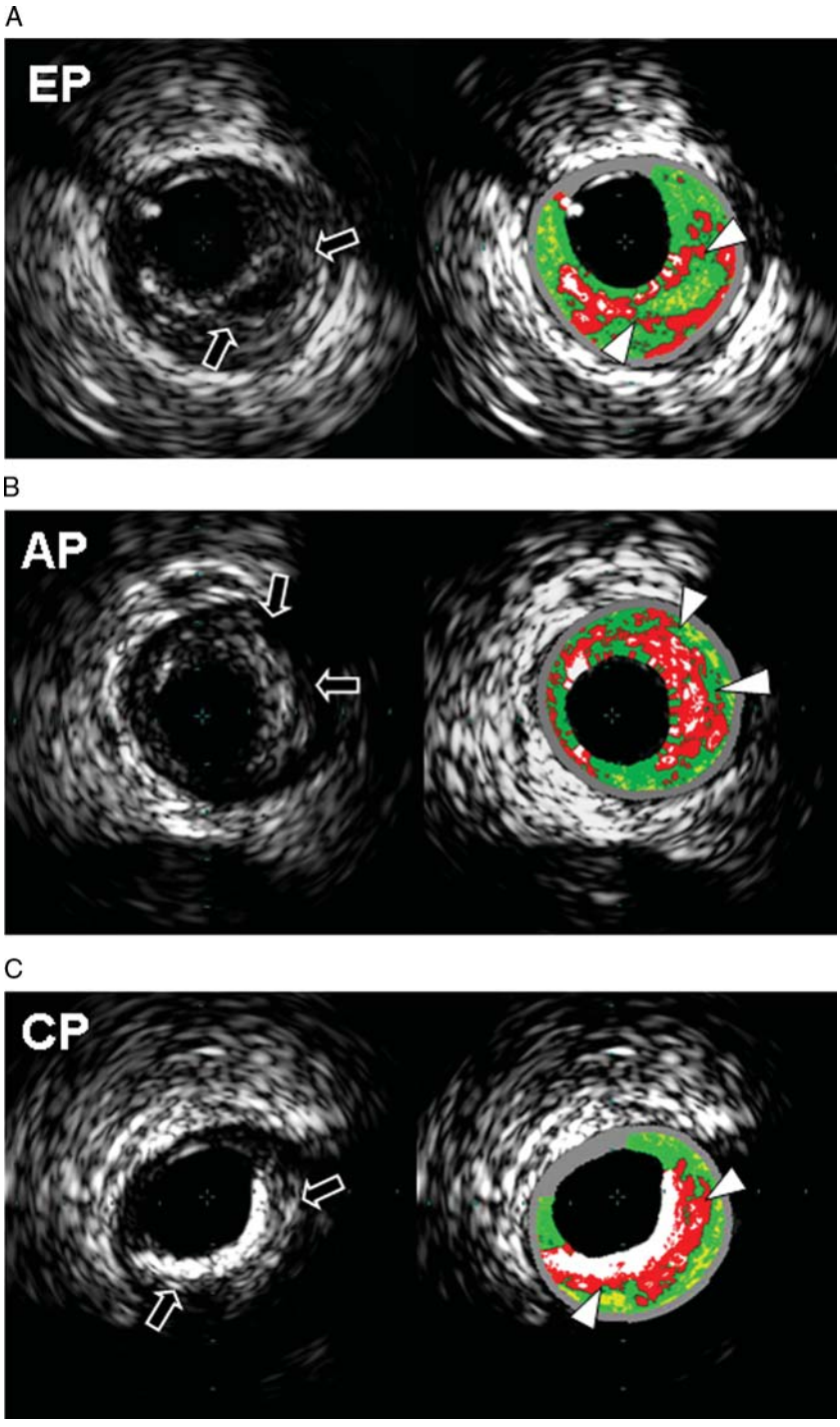

Figure 4 Representative greyscale-intravascular ultrasound and corresponding virtual histology-intravascular ultrasound images. (*A*) Echolucent plaque (EP) appears as 'black area' (arrow) in the greyscale-intravascular ultrasound image. The corresponding virtual histology-intravascular ultrasound shows mixture of fibrofatty (light green) and fibrous tissue (dark green) (white triangle) surrounded by necrotic core (red) indicating thin-cap fibroatheroma. Note that the necrotic core surrounds, but is not part, of the echolucent zone. (*B*) Attenuated plaque (AP) shows non-calcified plaque with attenuation (arrow) in the greyscale-intravascular ultrasound image. The corresponding virtual histology-intravascular ultrasound shows confluent necrotic core abutting the lumen, indicating virtual histology-thin-cap fibroatheroma. (*C*) Calcified plaque (CP) shows hyperechoic plaque with acoustic shadow (arrow). The corresponding virtual histology-intravascular ultrasound shows thick calcified cap with confluent necrotic core behind dense calcium (white), indicating calcified thick-cap FA.

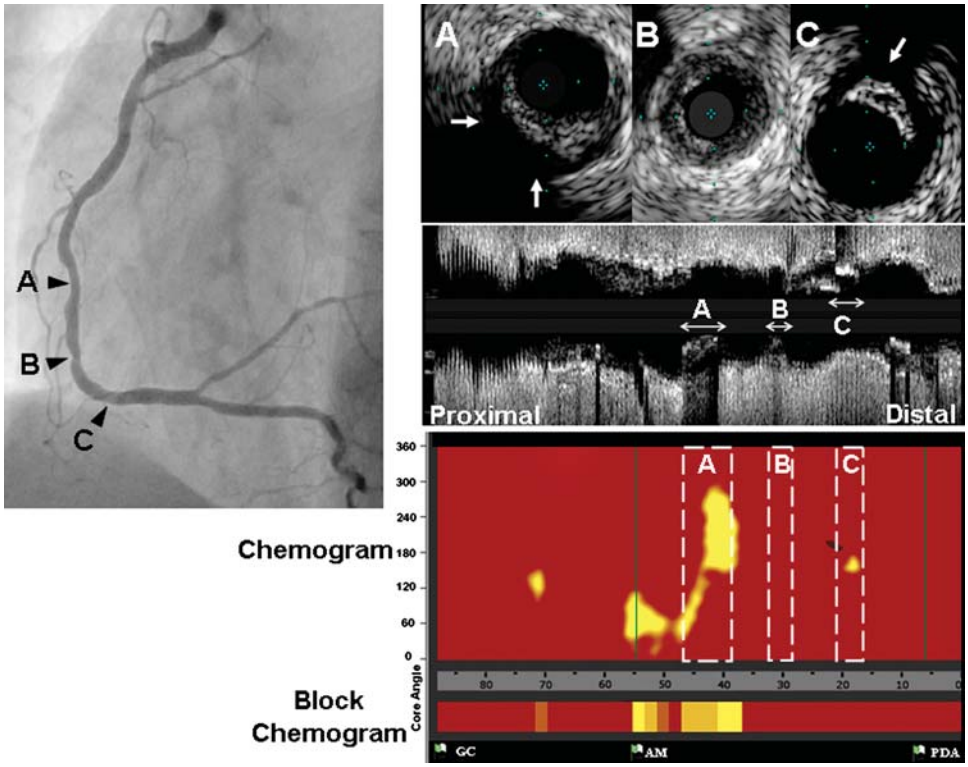

Figure 5 Representative near-infrared spectroscopy and corresponding angiogram and intravascular ultrasound images. 'A', 'B', and 'C' represent the same anatomic locations within the right coronary angiogram (left panel), greyscale-intravascular ultrasound (right top panel, cross-sectional view; right middle panel, longitudinal view), and near-infrared spectroscopy (right bottom panel). In the angiogram, there is a mild lesion at 'A', a significant stenosis at 'B', and minimal luminal irregularity at 'C'. In the greyscale-intravascular ultrasound, 'A' shows a typical attenuated plaque (white arrow), with the corresponding near-infrared spectroscopy region of interest showing extensive, circumferential lipid core plaque (yellow) in the 'chemogram' and yellow and tan blocks in the 'block chemogram'. In the greyscale-intravascular ultrasound study, 'B' shows a control plaque with no attenuation, echolucency, or calcification with the corresponding near-infrared spectroscopy 'chemogram' and 'block chemogram' containing only red, indicating low probability of lipid core. Finally, in the greyscale-intravascular ultrasound, 'C' shows calcified plaque (white arrow); the corresponding near-infrared spectroscopy 'chemogram' shows only a little yellow, whereas the 'block chemogram' contains only red blocks, indicating a low probability of lipid core plaque.

Although 75.0% of echolucent plaques were classified as VH-FAs, VH-NC was seen *surrounding* an echolucent zone, but not *within any* echolucent zone (*Figure 4*); and echolucent zones themselves contained mostly FT (6.2%), FF (37.5%), or a combination (56.3%). Echolucent plaques had significantly more VH-derived TCFAs (56.3 vs. 20.0%, $P = 0.023$) and a slightly higher maximum %NC [26.8% (15.9–34.8%) vs. 20.7% (14.3–25.6%), $P = 0.090$] when compared with control plaques.

On NIRS analysis, 75.0% of echolucent plaques contained lipid core; however, because NIRS did not provide structural information, it was not clear whether NIRS-detected lipid was within or surrounding the area that appeared echolucent on greyscale-IVUS imaging. Echolucent plaques had significantly higher NIRS-derived LCBI ($P = 0.008$) and mean angle ($P = 0.009$) when compared with control plaques (*Figure 6*).

Calcified plaques

VH analysis showed that in the calcified plaque group, all confluent DC had confluent 'NC' (range 16.0–41.2%) coexisting with calcium (*Figure 4*) with a significant positive correlation between the volume of DC vs. NC (Rho = 0.91, $P < 0.001$), %DC vs. %NC (Rho = 0.66, $P < 0.001$), or maximum %DC vs. maximum %NC (Rho = 0.70, $P < 0.001$). The %NC of calcified plaques was greater than that of control plaques (*Figure 3*, $P < 0.001$). All 41 greyscale-IVUS calcified plaques (arc >90°) were classified as calcified VH-FA with NC that measured 26.0% (IQR 22.1–31.3%). On NIRS analysis, we found that 58.5% of them contained lipid core. Lipid core burden index of calcified plaques was similar to that of control plaques (*Figure 6*).

Virtual histology-intravascular ultrasound vs. near-infrared spectroscopy findings

Since both VH-IVUS and NIRS were developed to detect lipidic necrotic regions within atherosclerotic plaques, we further compared VH-IVUS-derived vs. NIRS-derived parameters. Overall, the relation between VH-derived %NC vs. NIRS-derived LCBI was not significant (Rho = 0.16, $P = 0.110$). However, when lesions were separated according to greyscale-IVUS morphology,

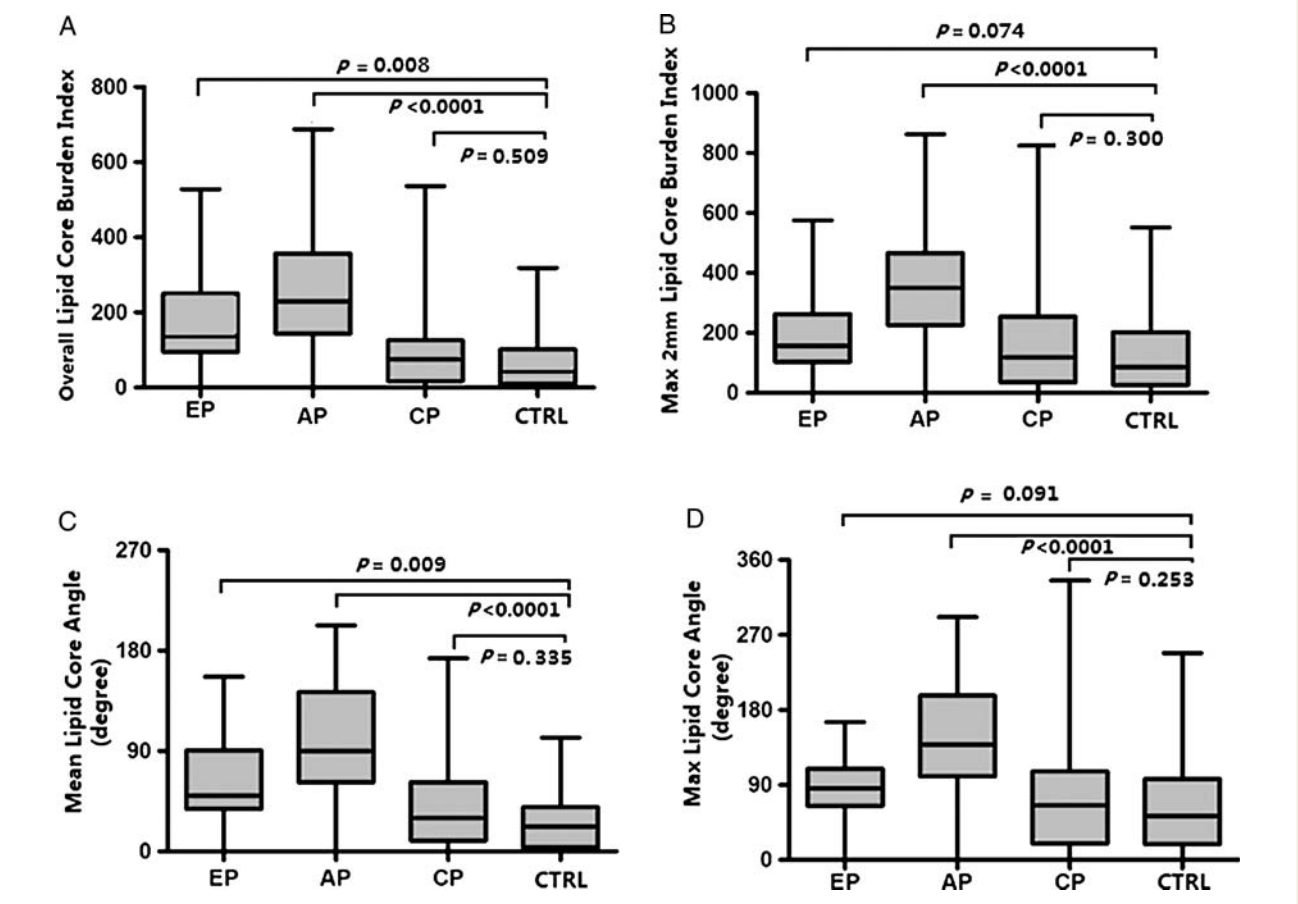

Figure 6 Relationship between greyscale-intravascular ultrasound plaque types and near-infrared spectroscopy findings. (*A*–*D*) Lipid core burden index (A), maximum 2 mm LCBI (lipid core burden index) (B), mean angle (C), and maximum angle (D) of lipid core in echolucent plaque (EP), attenuated plaque (AP), calcified plaque (CP) groups were compared with those in the control plaque (CTRL) group.

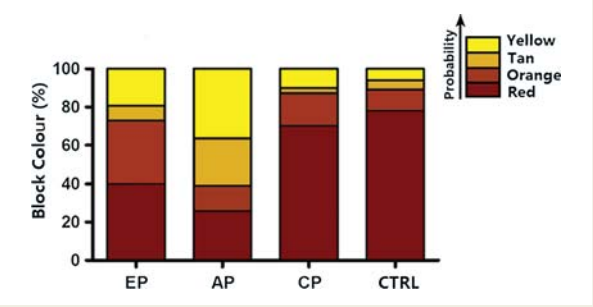

Figure 7 Percentages of colour blocks in near-infrared spectroscopy block chemogram. Percentages of different colour blocks within the region of interest in near-infrared spectroscopy 'block chemogram' among echolucent plaques (EP), attenuated plaques (AP), calcified plaques (CP), and control plaques (CTRL). These four colours (yellow, tan, orange, and red) indicate the probability of lipid core as described in Methods.

a significant positive relationship was found between VH-derived %NC vs. NIRS-derived LCBI (Rho = 0.50, $P = 0.006$) and between VH-derived maximum %NC and NIRS-derived maximum 2 mm LCBI (Rho = 0.40, $P = 0.037$) in attenuated plaques. Within the echolucent plaque group, there was a borderline correlation between VH-derived %NC vs. NIRS-derived LCBI (Rho = 0.42, $P = 0.076$) and a significant positive correlation between VH-derived maximum %NC vs. NIRS-derived maximum 2 mm LCBI (Rho = 0.49, $P = 0.048$). We did not find any correlations between VH-derived %NC vs. NIRS-derived LCBI (Rho = −0.18, $P = 0.316$) or between maximum %NC vs. maximum 2 mm LCBI (Rho = −0.06, $P = 0.681$) within the calcified plaque group. The correlation between VH-IVUS %NC vs. NIRS-derived LCBI in overall non-calcified plaques was significant (Rho = 0.51, $P = 0.001$) (*Figure 8*). Similar results were seen when comparing the mean and maximum angles of the NC (VH-IVUS) and lipid core (NIRS) (data not shown).

Plaque characteristics in acute coronary syndrome vs. non-acute coronary syndrome patients and among the three coronary arteries

Echolucent plaques (18.5 vs. 7.8%, $P = 0.065$) and attenuated plaques (34.6 vs. 18.4%, $P = 0.033$) were more common in ACS than in stable angina, with no difference in the frequency of calcified plaques between ACS and stable angina (31.5 vs. 31.2%; $P =$

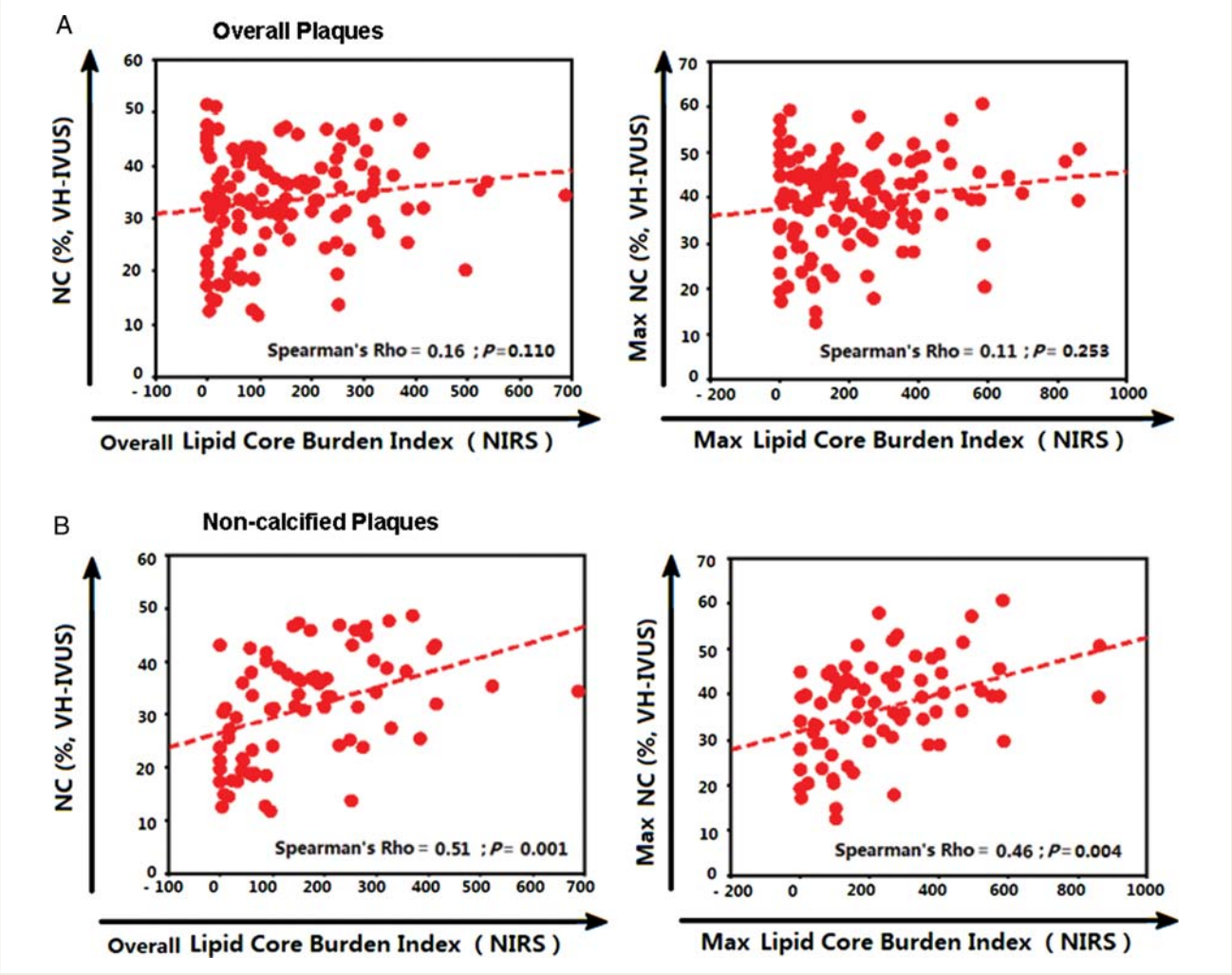

Figure 8 Correlation between near-infrared spectroscopy-derived and virtual histology-intravascular ultrasound-derived parameters. Spearman's rank correlation between lipid core burden index measured by near-infrared spectroscopy and %NC measured by virtual histology-intravascular ultrasound, or maximum 2 mm LCBI (lipid core burden index) and maximum %NC in the overall plaques (*A*) and non-calcified plaques (*B*).

0.811). The percentage of NC [23.9% (21–30.4%) vs. 20.1% (11.3–29.1%), $P = 0.028$] was higher in ACS than in stable angina, with no difference in the percentage of FT [48.5% (42.0–57.4%) vs. 49.5% (40.4–64.6%), $P = 0.243$], FF [13.2% (7.1–20.7%) vs. 9.9% (6.9–15.6%), $P = 0.081$], and DC [9.0% (2.8–20%) vs. 11.7% (6.5–19.6%), $P = 0.115$] between ACS and stable angina. Near-infrared spectroscopy-derived LCBI [131.6 (31.9–278.8) vs. 87.0 (21.4–152.2), $P = 0.020$], maximum 2 mm LCBI [204.9 (57.5–400.9) vs.135.9 (67.8–249.3), $P = 0.056$], and mean angle [57.0° (15.9–102.6°) vs. 33.8° (13.5–64.9°), $P = 0.018$] and maximum angle [94.2° (32–160°) vs. 65.5° (35.3–101.3°), $P = 0.042$] of lipid core were higher in ACS than in stable angina.

There was only a weak trend for a correlation between VH-derived %NC and NIRS-derived LCBI when analysis was performed in ACS patients (Rho = 0.24, $P = 0.097$), but there was no correlation in stable angina patients (Rho = 0.08, $P = 0.270$). However, the correlation between VH-IVUS %NC vs. NIRS-derived LCBI in non-calcified plaques was significant in both ACS (Rho = 0.56, $P = 0.001$) and stable angina subgroups (Rho = 0.41, $P = 0.006$). The correlation between VH-IVUS %NC vs. NIRS-derived LCBI disappeared in calcified plaques in both ACS (Rho = −0.22, $P = 0.534$) and stable angina subgroups (Rho = −0.08, $P = 0.232$). Similarly, when data were analysed by artery, the correlation between VH-IVUS %NC and NIRS-derived LCBI was significant in non-calcified plaques in the LAD (Rho = 0.56, $P = 0.001$), LCX (Rho = 0.50, $P = 0.015$) and RCA (Rho = 0.45, $P = 0.008$), but was not significant in calcified plaques in the LAD (Rho = −0.26, $P = 0.102$), LCX (Rho = −0.15, $P = 0.583$) and RCA (Rho = −0.08, $P = 0.642$).

Reproducibility of plaque type classification

Interobserver variability for plaque type classification was validated in 101 lesions from 51 randomly selected vessels. Blinded analyses were repeated by the first observer after an interval of 12 weeks

(intraobserver variability). The reproducibility of plaque type classification was assessed by kappa (κ) statistical analysis that corrects the chance of simple agreement and accounts for systematic observer bias. Interobserver agreement was moderate in the assessment of echolucent plaque ($\kappa = 0.733$, 95% CI 0.547–0.919) and good in the assessment of attenuated plaque ($\kappa = 0.894$, 95% CI 0.842–0.946); calcified plaque ($\kappa = 0.941$, 95% CI 0.907–0.975); and VH-IVUS phenotype [VH-TCFA ($\kappa = 0.832$, 95% CI 0.703–0.961), ThCFA ($\kappa = 0.840$, 95% CI 0.734–0.946), and PIT ($\kappa = 0.935$, 95% CI 0.890–0.980)]. Intraobserver variability yielded good concordance for echolucent plaque ($\kappa = 0.772$, 95% CI 0.580–0.964); attenuated plaque ($\kappa = 0.914$, 95% CI 0.865–0.963); calcified plaque ($\kappa = 0.960$, 95% CI 0.932–0.988); and VH-IVUS phenotype [VH-TCFA ($k = 0.866$, 95% CI 0.753–0.979), ThCFA ($\kappa = 0.859$, 95% CI 0.760–0.958), and PIT ($\kappa = 0.929$, 95% CI 0.878–0.981)].

Discussion

Our current knowledge about coronary plaque characteristics is largely obtained from *ex vivo* postmortem studies of lesions at the almost end of the coronary disease spectrum. In this *in vivo* comparison of tissue characterization of human coronary plaques using NIRS and greyscale and VH-IVUS, important findings were: (i) greyscale-IVUS-detected attenuated and echolucent plaques indicated the presence of NIRS-detected lipid core; (ii) most (93.5%) attenuated plaques contained confluent NC and were classified as VH-derived FA; (iii) although 75.0% of echolucent plaques were classified as VH-FAs, VH-NC was seen *surrounding* an echolucent zone, but not *within any* echolucent zone; (iv) all calcified plaques (arc >90°) contained >10% NC and were classified as VH-FA, whereas 58.5% contained NIRS-detected lipid core; (v) A positive relationship between VH-derived %NC and NIRS-derived LCBI was found in non-calcified plaques but not in calcified plaques.

Echolucent and attenuated plaques

Although conventional greyscale-IVUS is widely used during interventional procedures, several special greyscale-IVUS images—i.e. echolucent plaques and attenuated plaques—are still incompletely understood. Several small *in vitro* studies of echolucent and attenuated plaques yielded conflicting results.[15–19] For example, echolucent components detected by greyscale-IVUS have been related to high lipid content in some histological studies,[12,15] but to non-lipid components such as smooth muscle cells in other studies.[16,17] Attenuated plaque has also been variously related to cholesterol clefts, microcalcification, or organized thrombus.[18–20] In our study, tissue characterization by NIRS offered an *in vivo* opportunity to assess the chemical composition of echolucent and attenuated plaques. The NIRS findings suggested that these greyscale-IVUS characteristics were related to lipid content. In the NIRS 'block chemogram', the probability of lipid core was highest in attenuated plaques, followed by echolucent plaques.

These *in vivo* findings have clinical implications. Ultrasonic attenuation from non-calcified plaques (attenuated plaques) may indicate a large lipid/NC, whereas an intraplaque echolucent zone (echolucent plaques) may indicate a smaller lipid/NC.

Assessment of lipidic/necrotic core

A positive relationship between the NIRS-derived LCBI and VH-derived %NC was found in non-calcified plaques, but not in calcified plaques. The accuracy of VH-IVUS assessment of plaque composition behind calcium, especially NC, remains actively debated.[20–22] Highly calcified lesions might be an anatomical limitation to IVUS radiofrequency data analysis. It is unclear how often the VH-derived signals behind calcium are mostly noise and how often they contain useful data. Several investigators have shown that VH-IVUS of calcium can include a surrounding red halo that is part of the calculation of lesion NC, but that is most probably an artefact as has been suggested by Shin *et al.*[23,24]

Our results suggested that VH-IVUS might overestimate NC in the presence of heavy calcium. First, all calcified plaques (arc >90°) had >10% confluent VH-derived NC (range 16.0–41.2%) coexisting with calcium and were classified as VH-FAs. Second, significant and strong positive correlations between all parameters of DC and NC were found in the calcified plaque group, but not in other groups. Pathological studies have shown that not all calcified plaques contain NC. Calcium could deposit either within or around a necrotic region, resulting in the formation of a calcified FA (FA with calcified core); alternatively, calcium could deposit at sites of fibrous collagenous tissue, resulting in the formation of calcified fibrous plaque (calcified plaque without adjacent lipid/necrosis).[4,13,25] Absolute or relative amounts of VH-derived NC have been used as a risk stratification indicator for patients with coronary artery disease.[26] Our results suggested that caution should be taken in the VH-IVUS assessment of NC in vessels with heavy calcification, as has been demonstrated by a study using stent metal to simulate the addition of calcium to a lesion.[23]

VH-IVUS overestimation of NC content in the presence of calcification could also explain the discrepancy between VH-IVUS and NIRS findings in our study. Similar mean and maximum percentages of NC were found by VH-IVUS, but significantly lower mean and maximum LCBI values were shown by NIRS in calcified plaques compared with attenuated plaques. In addition, there was no correlation between VH-derived %NC and NIRS-derived LCBI in calcified plaques. Near-infrared spectroscopy, unlike ultrasound, assesses chemical composition based on near-infrared light absorption and scatter. Necropsy validation data have demonstrated that NIRS can differentiate calcified plaques containing a lipid core, from calcified fibrotic plaques that do not contain a lipid core.[4] In the current *in vivo* study, 58.5% of greyscale-IVUS calcified plaques contained NIRS-derived lipid core while all of them had >10% VH-IVUS NC. A study performed at almost the same time as the current study also compared NIRS and VH and showed that the overall correlation between the relative VH-NC content and the values of the NIRS block chemogram was weak,[27] similar to the current study. However, excluding calcified lesions from the analysis did not improve, but rather worsened the correlation. Several important differences between two studies might contribute to this disagreement. First, the 'plaque' in the study by Brugaletta *et al.*[27] was defined according to the NIRS chemogram blocks, not greyscale-IVUS. Second, the 'calcified plaque' in the study by Brugaletta *et al.*[27] was defined as >10% of average VH-DC content for a given VH segment matched to a

2 mm chemogram block and not based on the greyscale-IVUS criteria as in the current study. Third, in the study by Brugaletta *et al*., NIRS was compared with the VH-derived %NC using the 'chemogram block probability' defined as the probability of LCP displayed in the chemogram block rather than using the LCBI. The NIRS 'block chemogram' provides only a summary of the data in every 2 mm segment and does not indicate individual pixel data or the location of a measurement in the circumferential dimension, and, therefore, correlating 'chemogram block probability' to the VH-derived %NC might not be the optimal approach.

Clinical implications

In the present study, we showed that echolucent and attenuated plaques were more frequent in ACS than in stable angina, with no difference in the frequency of calcified plaques between ACS and stable angina. Tissue characterization by NIRS and VH-IVUS in the present study suggested that echolucent and attenuated plaques were representative of lipid/NC-containing plaques. In previous studies, although the mechanisms were unclear, both echolucent plaques and attenuated plaques have been associated with distal embolization during PCI, especially PCI of patients presenting with ACS. Similarly, in seven studies, VH-derived NC has also been associated with distal embolization (using a variety of endpoints) during PCI, again especially PCI of patients presenting with ACS.[26,28,29] Finally, in one published NIRS study, a large amount of lipid plaque has also been associated with distal embolization during PCI, leading to the randomized CANARY(Coronary Assessment by Near-infrared of Atherosclerotic Rupture-prone Yellow) trial comparing distal protection vs. no distal protection in patients with an LCBI >600.[29] The current three-way greyscale-IVUS, VH-IVUS, and NIRS comparison links these observations.

Study limitations

First, although data in our study are prospectively collected and blindly analysed, the sample size (131 plaques in 66 vessels) was relatively small. Second, we did not assess very severe stenoses because NIRS and IVUS were usually performed after pre-dilation of such lesions. Third, we could not exclude the possibility of a mismatch in the analysis segments, leading to inaccuracies in the registration of segments between the different technologies. The development of NIRS/IVUS combination catheter, in part, addressed this issue. Fourth, the VH-IVUS identification of a TCFA is inferential because a thin-fibrous cap is below the resolution of IVUS; however, a VH-TCFA was a predictor of events in PROSPECT.[11] In addition, because the NIRS system used in this study did not provide structural information, we were only able to compare entire cross-sections between spectroscopy and ultrasound and not individual regions of interest. Finally, our findings from the coronary arteries of *in vivo* patients lack a direct comparison with histopathology. *Ex vitro* histological studies in human coronary autopsy specimens are needed in order to further confirm such *in vivo* findings in living patients.

Conclusion

Combining NIRS with IVUS contributes to the understanding of plaque characterization *in vivo*. An NIRS/IVUS (optical/acoustic) combination catheter, which allows co-registration of coronary anatomy and chemical composition, has been developed and is currently undergoing pre-clinical and early clinical evaluation.[30] Further studies are warranted to determine whether combining NIRS and IVUS techniques will enhance the assessment of high-risk plaque to predict outcomes in patients with coronary artery disease.

Conflict of interest: G.S.M. reports receiving consulting fees from Boston Scientific and Volcano and research/grant support from Boston Scientific, InfraReDx, and Volcano. G.W.S. reports being an advisory board for Boston Scientific and Abbott Vascular, and a consultant for Medtronic, Volcano, and InfraRedx. E.S.B. reports receiving speaker honoraria from St Jude Medical and Terumo, and research support from Abbott Vascular. S.B. reports receiving speaker honoraria from St Jude Medical, Medtronic, and Johnson & Johnson and research support from Boston Scientific and The Medicines Company. B.M. reports being an advisory board for InfraRedx, Abiomed, and Medtronic, and a consultant for Abbott Vascular and St Jude Medical. A.M. reports receiving research grants from Boston Scientific and lecture fee from Volcano. J.P. reports receiving research grants from Boston Scientific China.

References

1. Schoenhagen P, Nair A, Nicholls S, Vince G. Assessment of plaque burden and plaque composition using intravascular ultrasound. In: Naghavi M (ed), *Asymptomatic Atherosclerosis: Pathophysiology, Detection and Treatment*. Part 5. Humana Press; 2010. p483–493.
2. Garcia-Garcia HM, Costa MA, Serruys PW. Imaging of coronary atherosclerosis: intravascular ultrasound. *Eur Heart J* 2010;**31**:2456–2469.
3. Moreno PR, Lodder RA, Purushothaman KR, Charash WE, O'Connor WN, Muller JE. Detection of lipid pool, thin fibrous cap, and inflammatory cells in human aortic atherosclerotic plaques by near-infrared spectroscopy. *Circulation* 2002;**105**:923–927.
4. Gardner CM, Tan H, Hull EL, Lisauskas JB, Sum ST, Meese TM, Jiang C, Madden SP, Caplan JD, Burke AP, Virmani R, Goldstein J, Muller JE. Detection of lipid core coronary plaques in autopsy specimens with a novel catheter-based near-infrared spectroscopy system. *JACC Cardiovasc Imaging* 2008;**1**:638–648.
5. Waxman S, Dixon SR, L'Allier P, Moses JW, Petersen JL, Cutlip D, Tardif JC, Nesto RW, Muller JE, Hendricks MJ, Sum ST, Gardner CM, Goldstein JA, Stone GW, Krucoff MW. *In vivo* validation of a catheter-based near-infrared spectroscopy system for detection of lipid core coronary plaques: initial results of the SPECTACL study. *JACC Cardiovasc Imaging* 2009;**2**:858–868.
6. Yamagishi M, Terashima M, Awano K, Kijima M, Nakatani S, Daikoku S, Ito K, Yasumura Y, Miyatake K. Morphology of vulnerable coronary plaque: insights from follow-up of patients examined by intravascular ultrasound before an acute coronary syndrome. *J Am Coll Cardiol* 2000;**35**:106–111.
7. Endo M, Hibi K, Shimizu T, Komura N, Kusama I, Otsuka F, Mitsuhashi T, Iwahashi N, Okuda J, Tsukahara K, Kosuge M, Ebina T, Umemura S, Kimura K. Impact of ultrasound attenuation and plaque rupture as detected by intravascular ultrasound on the incidence of no-reflow phenomenon after percutaneous coronary intervention in ST-segment elevation myocardial infarction. *JACC Cardiovasc Interv* 2010;**3**:540–549.
8. Kimura S, Kakuta T, Yonetsu T, Suzuki A, Iesaka Y, Fujiwara H, Isobe M. Clinical significance of echo signal attenuation on intravascular ultrasound in patients with coronary artery disease. *Circ Cardiovasc Interv* 2009;**2**:444–454.
9. Mintz GS, Pichard AD, Popma JJ, Kent KM, Satler LF, Bucher TA, Leon MB. Determinants and correlates of target lesion calcium in coronary artery disease: a clinical, angiographic and intravascular ultrasound study. *J Am Coll Cardiol* 1997;**29**:268–274.
10. Kubo T, Maehara A, Mintz GS, Doi H, Tsujita K, Choi SY, Katoh O, Nasu K, Koenig A, Pieper M, Rogers JH, Wijns W, Böse D, Margolis MP, Moses JW, Stone GW, Leon MB. The dynamic nature of coronary artery lesion morphology assessed by serial virtual histology intravascular ultrasound tissue characterization. *J Am Coll Cardiol* 2010;**55**:1590–1597.
11. Stone GW, Maehara A, Lansky AJ, de Bruyne B, Cristea E, Mintz GS, Mehran R, McPherson J, Farhat N, Marso SP, Parise H, Templin B, White R, Zhang Z, Serruys PW; PROSPECT Investigators. A prospective natural-history study of coronary atherosclerosis. *N Engl J Med* 2011;**364**:226–235.

12. Mintz GS, Nissen SE, Anderson WD, Bailey SR, Erbel R, Fitzgerald PJ, Pinto FJ, Rosenfield K, Siegel RJ, Tuzcu EM, Yock PG. American College of Cardiology Clinical Expert Consensus Document on Standards for Acquisition, Measurement and Reporting of Intravascular Ultrasound Studies (IVUS). A report of the American College of Cardiology Task Force on Clinical Expert Consensus Documents. *J Am Coll Cardiol* 2001;**37**:1478–1492.
13. García-García HM, Mintz GS, Lerman A, Vince DG, Margolis MP, van Es GA, Morel MA, Nair A, Virmani R, Burke AP, Stone GW, Serruys PW. Tissue characterisation using intravascular radiofrequency data analysis: recommendations for acquisition, analysis, interpretation and reporting. *EuroIntervention* 2009;**5**:177–189.
14. Guo N, Maehara A, Mintz GS, He Y, Xu K, Wu X, Lansky AJ, Witzenbichler B, Guagliumi G, Brodie B, Kellett MA Jr, Dressler O, Parise H, Mehran R, Stone GW. Incidence, mechanisms, predictors, and clinical impact of acute and late stent malapposition after primary intervention in patients with acute myocardial infarction: an intravascular ultrasound substudy of the Harmonizing Outcomes with Revascularization and Stents in Acute Myocardial Infarction (HORIZONS-AMI) trial. *Circulation* 2010;**122**:1077–1084.
15. Prati F, Arbustini E, Labellarte A, Dal Bello B, Sommariva L, Mallus MT, Pagano A, Boccanelli A. Correlation between high frequency intravascular ultrasound and histomorphology in human coronary arteries. *Heart* 2001;**85**:567–570.
16. Hiro T, Leung CY, De Guzman S, Caiozzo VJ, Farvid AR, Karimi H, Helfant RH, Tobis JM. Are soft echoes really soft? Intravascular ultrasound assessment of mechanical properties in human atherosclerotic tissue. *Am Heart J* 1997;**133**:1–7.
17. Bruining N, Verheye S, Knaapen M, Somers P, Roelandt JR, Regar E, Heller I, de Winter S, Ligthart J, Van Langenhove G, de Feijter PJ, Serruys PW, Hamers R. Three-dimensional and quantitative analysis of atherosclerotic plaque composition by automated differential echogenicity. *Catheter Cardiovasc Interv* 2007;**70**:968–978.
18. Hara H, Tsunoda T, Moroi M, Kubota T, Kunimasa T, Shiba M, Wada M, Tsuji T, Iijima R, Nakajima R, Yoshitama T, Nakamura M. Ultrasound attenuation behind coronary atheroma without calcification: mechanism revealed by autopsy. *Acute Card Care* 2006;**8**:110–112.
19. Yamada R, Okura H, Kume T, Neishi Y, Kawamoto T, Watanabe N, Toyota E, Yoshida K. Histological characteristics of plaque with ultrasonic attenuation: a comparison between intravascular ultrasound and histology. *J Cardiol* 2007;**50**:223–228.
20. Maehara A, Mintz GS, Weissman NJ. Advances in intravascular imaging. *Circ Cardiovasc Interv* 2009;**2**:482–490.
21. Carlier SG, Mintz GS, Stone GW. Imaging of atherosclerotic plaque using radiofrequency ultrasound signal processing. *J Nucl Cardiol* 2006;**13**:831–840.
22. Murray SW, Palmer ND. What is behind the calcium? The relationship between calcium and necrotic core on virtual histology analyses. *Eur Heart J* 2009;**30**:125.
23. Sales FJ, Falcão BA, Falcão JL, Ribeiro EE, Perin MA, Horta PE, Spadaro AG, Ambrose JA, Martinez EE, Furuie SS, Lemos PA. Evaluation of plaque composition by intravascular ultrasound virtual histology: the impact of dense calcium on the measurement of necrotic tissue. *EuroIntervention* 2010;**6**:394–399.
24. Shin ES, Garcia-Garcia HM, Ligthart JM, Witberg K, Schultz C, van der Steen AF, Serruys PW. *In vivo* findings of tissue characteristics using iMap™ IVUS and Virtual Histology™ IVUS. *EuroIntervention* 2011;**6**:1017–1019.
25. Virmani R, Kolodgie FD, Burke AP, Farb A, Schwartz SM. Lessons from sudden coronary death: a comprehensive morphological classification scheme for atherosclerotic lesions. *Arterioscler Thromb Vasc Biol* 2000;**20**:1262–1275.
26. Kawaguchi R, Oshima S, Jingu M, Tsurugaya H, Toyama T, Hoshizaki H, Taniguchi K. Usefulness of virtual histology intravascular ultrasound to predict distal embolization for ST-segment elevation myocardial infarction. *J Am Coll Cardiol* 2007;**50**:1641–1646.
27. Brugaletta S, Garcia-Garcia HM, Serruys PW, de Boer S, Ligthart J, Gomez-Lara J, Witberg K, Diletti R, Wykrzykowska J, van Geuns RJ, Schultz C, Regar E, Duckers HJ, van Mieghem N, de Jaegere P, Madden SP, Muller JE, van der Steen AF, van der Giessen WJ, Boersma E. NIRS and IVUS for characterization of atherosclerosis in patients undergoing coronary angiography. *JACC Cardiovasc Imaging* 2011;**4**:647–655.
28. Hong YJ, Jeong MH, Choi YH, Ko JS, Lee MG, Kang WY, Lee SE, Kim SH, Park KH, Sim DS, Yoon NS, Youn HJ, Kim KH, Park HW, Kim JH, Ahn Y, Cho JG, Park JC, Kang JC. Impact of plaque components on no-reflow phenomenon after stent deployment in patients with acute coronary syndrome: a virtual histology-intravascular ultrasound analysis. *Eur Heart J* 2011;**32**:2059–2066.
29. Kawamoto T, Okura H, Koyama Y, Toda I, Taguchi H, Tamita K, Yamamuro A, Yoshimura Y, Neishi Y, Toyota E, Yoshida K. The relationship between coronary plaque characteristics and small embolic particles during coronary stent implantation. *J Am Coll Cardiol* 2007;**50**:1635–1640.
30. Schultz CJ, Serruys PW, van der Ent M, Ligthart J, Mastik F, Garg S, Muller JE, Wilder MA, van de Steen AF, Regar E. First-in-man clinical use of combined near-infrared spectroscopy and intravascular ultrasound: a potential key to predict distal embolization and no-reflow?. *J Am Coll Cardiol* 2010;**56**:314.